LIMNOLOGY and OCEANOGRAPHY

ASLO

Limnol. Oceanogr. 9999, 2025, 1–18

doi: 10.1002/lno.70021

RESEARCH ARTICLE

Springtime upwelling conditions influence microbial communities and dissolved thiamin compounds in the California Current Ecosystem

Kelly C. Shannon,[1] Gillian St. John,[1] Robin Gould,[2] Christopher Hartzell,[2] Hailey Matthews,[1] Elizabeth J. Brennan,[1] Luis M. Bolaños,[3] Steven T. Lindley,[4] John C. Field,[4] Nate Mantua,[4] Rachel Johnson,[4,5] Carson Jeffres,[5] Frederick S. Colwell,[1,6] Christopher P. Suffridge [1]*

[1]Department of Microbiology, Oregon State University, Corvallis, Oregon, USA; [2]Department of Biochemistry and Biophysics, Oregon State University, Corvallis, OR, USA; [3]School of Biosciences, University of Exeter, Exeter, UK; [4]Southwest Fisheries Science Center, NOAA Fisheries, Santa Cruz, California, USA; [5]Center for Watershed Sciences, University of California Davis, Davis, California, USA; [6]College of Earth, Ocean, and Atmospheric Sciences, Oregon State University, Corvallis, Oregon, USA

Abstract

Understanding dissolved concentrations of the essential coenzyme thiamin (vitamin B_1) can provide insights into the biological controls on highly productive upwelling systems such as the California Current Ecosystem. To connect thiamin availability with microbial communities in the California Current Ecosystem, we measured concentrations of dissolved thiamin and its biochemically related moieties (thiamin congeners) and 16S rRNA gene-based microbial communities during the spring. We found that strong upwelling caused a depletion of dissolved thiamin precursor compounds and abiotic degradation products relative to periods of weak upwelling. Specific microbial taxa, including species of SAR11 ecotypes, *Candidatus* Nitrosopumilus, and SUP05 cluster, were also significantly enriched with strong upwelling. Our data provide evidence that alterations to microbial communities in the mixed layer that occur as a result of upwelling could constrain the availability of dissolved thiamin and its chemical congeners in the California Current Ecosystem.

Thiamin (vitamin B_1, or B_1) is an essential coenzyme for anabolic and catabolic central carbon metabolism (Zhang et al. 2016; Jurgenson et al. 2009). In marine ecosystems, the availability of intact thiamin (synthesized from its precursor compounds; unphosphorylated) and its biochemically related compounds (together referred to as thiamin congeners) play important roles in structuring microbial community composition (Suffridge et al. 2018). Microbial requirements for these compounds are prevalent in marine environments (Paerl et al. 2018b). This results in thiamin congeners being trafficked through the marine dissolved pool between thiamin prototrophic organisms that have the complete thiamin biosynthesis pathway and thiamin auxotrophic organisms that lack the complete thiamin biosynthesis pathway, and therefore must rely on exogenous sources of these compounds (Suffridge et al. 2020; Wienhausen et al. 2017; Bertrand and Allen 2012). Disruptions to the balance between microbial production and biotic and abiotic removal (e.g., cellular uptake or environmental degradation) of thiamin can result in a net accumulation or depletion, respectively of dissolved thiamin congeners in the water column (Suffridge et al. 2020). Evolutionary mechanisms for thiamin congener acquisition by auxotrophs are driven by the scarcity of these compounds in the dissolved pool and are used by microbes to compete for these limited resources in aquatic ecosystems (Sañudo-Wilhelmy et al. 2014; Kraft and Angert 2017; Gutowska et al. 2017).

Thiamin is biosynthesized through the ligation of its pyrimidine and thiazole moieties, 4-amino-5 hydroxymethyl-2-methylpyrimidine (HMP) and 5-(2-hydroxyethyl)-4-methyl-

*Correspondence: suffridc@oregonstate.edu

Associate editor: Hans-Peter Grossart

Data Availability Statement: All microbial sequence processing and data analysis scripts can be found here: https://github.com/ksmicrobe/CA_RL2103/tree/main. All sequencing data can be accessed with the following NCBI SRA BioProject ID: PRJNA1097642.

1,3-thiazole-2-carboxylic acid (cHET), respectively, which are solely produced by microbial biosynthesis (Jurgenson et al. 2009; Paerl et al. 2018a). The cleavage of thiamin through abiotic degradation mechanisms (Basant and Arnold 1973; Carlucci et al. 1969; Gold 1968) produces the thiazole degradation product, 4-methyl-5-thiazoleethanol (HET) and the pyrimidine degradation product, 4-amino-5-aminomethyl-2-methylpyrimidine (AmMP). Microbes use these thiamin congeners, in addition to thiamin itself, to supplement biosynthesis and cellular requirements (Croft et al. 2006; Wienhausen et al. 2022; Paerl et al. 2017). To assess environmental thiamin availability and its connection to microbial ecology, thiamin's metabolically relevant precursor compounds and abiotic degradation products must be simultaneously measured (Suffridge et al. 2017; Suffridge et al. 2020).

The composition of marine microbial communities can influence net thiamin congener production or removal from the dissolved pool, and cellular auxotrophy can influence which individual dissolved thiamin congeners are removed (Bittner et al. 2024). For example, many picoeukaryotic phytoplankton are thiazole auxotrophs that salvage extracellular cHET to synthesize thiamin (Paerl et al. 2017). Other algal groups such as *Cyanophyceae* and Stramenopiles contain species with complete thiamin biosynthesis pathways and may not require extracellular thiamin congeners (Monteverde et al. 2015; Sanudo-Wilhelmy et al. 2012). Further, many heterotrophic bacteria associated with algal blooms can be auxotrophic for thiamin precursors (cHET and HMP) and include *Flavobacteria* spp. (Suffridge et al. 2020), globally ubiquitous SAR11 species (Carini et al. 2014), and copiotrophic Gammaproteobacteria (Paerl et al. 2018b). Linking the compositional characteristics of marine microbial communities with thiamin congener measurements will allow us to connect taxonomic identities of bacteria, archaea, and algae with concentrations of the thiamin congeners that they cycle.

Dissolved thiamin congener concentrations have been measured across widespread marine ecosystems (Carini et al. 2014), but few studies have examined these compounds in Eastern Boundary Upwelling Systems (Monteverde et al. 2015, Sanudo-Wilhelmy et al. 2012), which greatly influence global ocean productivity and are disproportionately impacted by climate change (Bograd et al. 2023). The California Current Ecosystem (CCE) is a highly biologically productive Eastern Boundary Upwelling System that stretches from Vancouver Island, Canada, to Baja California, Mexico (Checkley and Barth 2009). Wind-driven upwelling in the CCE occurs following spring transitions between April and May and brings cold, nutrient-rich subsurface water into the euphotic zone, stimulating high levels of primary production (Huyer 1983; Venrick 2009; Hickey and Banas 2003). The intensification and relaxation of the winds that drive upwelling, and their interaction with coastal topography and bathymetry, create dynamic spatial and temporal oceanographic variability (Venrick 2009), which impacts the composition of coastal microbial communities throughout the water column (James et al. 2022) and likely dissolved thiamin congener concentrations.

Microbial communities in the CCE have been extensively studied (Countway et al. 2010; Venrick 2009; Santoro et al. 2010), yet associations between dissolved thiamin congener (thiamin, cHET, HET, HMP, and AmMP) concentrations and community compositions are unknown and could clarify why certain microbial populations are more successful than others. Our objective was therefore to determine how microbial community composition and dissolved thiamin congener concentrations couple with fundamental environmental properties (including upwelling) within an Eastern Boundary Upwelling System. Accordingly, water column microbial and dissolved thiamin congener samples were collected from depths spanning the surface to beneath the mixed layer between April and May 2021 along the central region of the CCE (Fig. 1a). We hypothesized that (1) springtime CCE microbial community composition influences dissolved thiamin congener availability due to upwelling-associated microbial community changes and elevated primary productivity, (2) upwelling-associated factors, including upwelling intensity and water column chemical and biological properties, correlate with microbial communities and dissolved thiamin congener concentrations, and (3) dissolved thiamin congener concentrations in the central CCE differ from those of previously measured marine environments because of the unique biological and upwelling conditions in these coastal habitats.

Methods

Sample collection and site description

Sample collection occurred aboard the National Oceanic and Atmospheric Administration Ship R/V *Reuben Lasker* during the 2021 annual Rockfish Recruitment and Ecosystem Assessment Survey (Field et al. 2021; Santora et al. 2021). Water samples for dissolved thiamin congeners and microbial community analyses were collected from four transect lines during the annual survey within the central region of the CCE (central CCE; between Cape Mendocino, CA and Point Conception, CA; Checkley and Barth 2009) (Fig. 1a). Sample lines were off Point Arena (Navarro), in the Gulf of the Farallones (Farallones), Monterey Bay (Monterey), and off Point Sur. Samples were collected at four depths per station (exact depths in Supporting Information Fig. S1). Exact sampling depths varied at each station and were selected in real time by observing oceanographic conditions (temperature, salinity, density, and chlorophyll *a*) during the conductivity, temperature, and depth (CTD) downcast to capture the surface, mixed layer, deep chlorophyll maximum (DCM; if present), and below the mixed layer. Navarro samples were collected on April 29th (stations 461 and 463) and April 30th (stations 464, 465, and 466); Farallones samples were collected on May 1st (stations

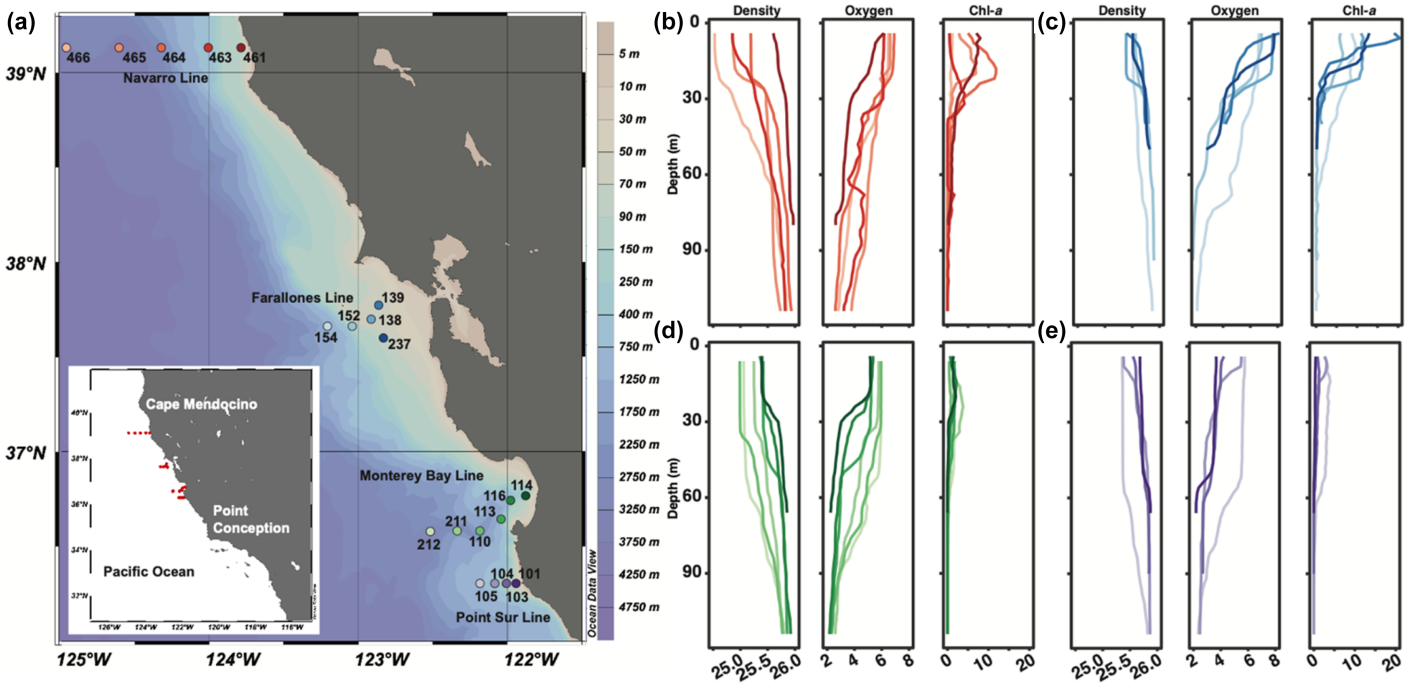

Fig. 1. Sample site map and environmental conditions. (**a**) Bathymetric map overlaid with the locations where samples were collected in the central transect of the California Current Ecosystem (S of Cape Mendocino; N of Point Conception). Coloration indicates water depth. Red points indicate individual stations sampled for four depths along each sampling line. Latitudes span the *y*-axis and longitudes span the *x*-axis. Publicly available upwelling measurements were retrieved based on each degree of latitude. Station profiles of density (kg m^{-3}), oxygen (ml L^{-1}), and chlorophyll *a* (mg L^{-1}) for the (b) Navarro, (c) Farallones, (d) Monterey, and (e) Point Sur lines. Lines are organized by high–low latitude and stations are organized from furthest–closest to the coast from top to bottom and light to dark color. Station colors within each line correspond to those depicted in panel (**a**).

138, 152, and 154) and May 13th (139 and 237); Monterey samples were collected on May 2nd (113, 114, and 116) and May 3rd (110, 211, and 212); and all Point Sur samples were collected on May 5th. Samples were collected as previously described (Suffridge et al. 2017; Suffridge et al. 2020) (Supplemental Methods). Sampling line-specific environmental factors in the central CCE include submarine canyons in Navarro and Monterey stations, which are sites of enhanced mixing, upwelling, and cross-shelf transport (Hickey 1995; Carter and Gregg 2002). Additionally, the Gulf of the Farallones is characterized by a broad, shallow shelf in an "upwelling shadow" that is sheltered from northerly winds and alongshore currents, with more persistent high temperature and chlorophyll signals as a result of the increased water retention (Steger et al. 2000; Vander Woude et al. 2006). These Farallones sites are also impacted by the San Francisco Bay plume, which can stimulate primary production from nutrient and dissolved organic matter transport from San Francisco Bay (Zhou et al. 2023).

Ship CTD data was used post-expedition to construct station temperature, density, salinity, oxygen, and chlorophyll *a* depth profiles for each station (Santora et al. 2021; Closek et al. 2019). Mixed layer depths of each station were calculated post-expedition based on CTD-derived temperature changes of 0.2°C from reference depths of 10 m (de Boyer Montégut et al. 2004). The DCM from each profile was visually determined based on fluorometric chlorophyll *a* depth profiles constructed from CTD data post-expedition following previous work (Cornec et al. 2021). Temporal examinations of upwelling intensity were performed with the coastal upwelling transport (CUTI) and biologically effective upwelling transport (BEUTI) indices (c.f., Jacox et al. 2018) (Supplemental Methods; https://oceanview.pfeg.noaa.gov/products/upwelling/cutibeuti). Upwelling intensity categories were defined based on the 25th and 75th percentiles of CUTI and biologically effective upwelling transport index values across all lines (0.71 and 2.20 m^2 water s^{-1}, respectively for CUTI; 14.44 and 48.66 mmol nitrate m^{-1} s^{-1}, respectively, for biologically effective upwelling transport index).

Dissolved thiamin congener analysis

Dissolved thiamin congeners were extracted from the seawater matrix as previously described (Suffridge et al. 2020; Suffridge et al. 2017). Briefly, Bondesil C_{18} resin (Agilent) was used for the solid-phase extraction. Compounds were then eluted using liquid chromatography mass spectrometry grade methanol, which was subsequently concentrated using a blow-down nitrogen drier (Glass Col). Hydrophobic organic compounds that were co-extracted by the solid-phase extraction were removed using a liquid-phase extraction with 1:1

volume of chloroform. Samples were then stored at −80°C until liquid chromatography mass spectrometry analysis. Sample analysis was conducted using liquid chromatography mass spectrometry as previously described (Suffridge et al. 2020) (Supplemental Methods) using an Applied Biosystems 4000 Q-Trap triple quadrupole mass spectrometer with an ESI interface coupled to a Shimadzu LC-20 AD liquid chromatograph. Applied Biosystems Analyst and ABSciex Multiquant software were used for instrument operation and sample quantification.

Water column microbial DNA lab methods and high-throughput sequencing

DNA was extracted from the Sterivex filters that were used for the filtration of dissolved thiamin congener samples, as previously described (Suffridge et al. 2023) (Supplemental Methods). The V3–V4 hypervariable region of the 16S rRNA gene was amplified by polymerase chain reaction (*see* PCR details in Supplemental Methods) with 515f (GTGYCAGCMGCCGCGGTAA) and 806r (GGACTACNVGGGTWTCTAAT) primers (Parada et al. 2016; Apprill et al. 2015). Purified and cleaned amplicons from all samples were then pooled to equimolar concentrations (25 ng DNA per sample) and sequenced at the Oregon State University Center for Quantitative Life Sciences facility with 2 × 250 bp Illumina MiSeq high-throughput sequencing. Read data output from MiSeq was demultiplexed, and primers were trimmed in-house by the Center for Quantitative Life Sciences.

Microbial data processing and analysis

Initial quality filtering (reads with average Phred score of < 20 dropped) and read quality visualization were performed with Trim Galore (v0.6.7), FastQC (v0.11.9), and MultiQC (v1.14; Ewels et al. 2016). All further bioinformatics and statistics work were performed in RStudio (v4.2.1; RStudio Team 2020). Processing of reads to amplicon sequence variants (ASVs) was performed in DADA2 (v1.24.0; Callahan et al. 2016). Reads were trimmed in DADA2 (Phred score threshold of 30) based on MultiQC quality reports, and pseudo-pooling was utilized for ASV assignment. Reads from each of the two MiSeq runs were processed separately for ASV assignment, and the resulting sequence tables were merged prior to taxonomic assignment (*see* Data Availability Statement for sequence processing script). Samples Navarro-465 and Farallones-138 at depths of 20 and 4 m, respectively, were unsuccessful in being sequenced and were removed from further microbial analyses.

Bacterial and archaeal ASV taxonomies were assigned with the Silva reference database (v138.1; Quast et al. 2013) and plastid taxonomy was assigned by aligning Chloroplast ASV sequences (as assigned by Silva) to the PhytoREF (Decelle et al. 2015) reference database (sequence headers modified to be used in DADA2; *see* Data Availability Statement for file). The decontam package (v1.16.0; Davis et al. 2018) was utilized to retrieve potential contaminant ASVs that showed up in the negative control samples. No ASVs were removed, and ASV presence in negative controls was attributed to well-to-well contamination from true samples in 96-well plates during polymerase chain reaction preparation (Minich et al. 2019). Further, negative controls displayed a lack of gel electrophoresis bands and low Qubit fluorometer DNA concentration values (< 1.0 ng μL^{-1}). The phyloseq package (v1.42.0; McMurdie and Holmes 2013) was utilized to construct a phyloseq object of bacteria, archaea, and plastid-assigned algae. Samples in the phyloseq object were normalized with total sum scaling (or proportions) for all further 16S analyses, other than differential abundance. Rarefaction was performed for Shannon diversity estimates. Differences in unrarefied and total sum scaling-normalized microbial communities (beta-diversity) were examined with Bray–Curtis dissimilarity, following the recommendations of McKnight et al. (2018). Permutational multivariate ANOVA analyses for group comparisons were performed with both rarefied and unrarefied phyloseq objects and yielded identical p values, indicating a low influence of rarefaction on between-group microbial community statistical results. All plots were made with the ggplot2 (v3.4.4; Wickham 2009) and ggpubr (v0.6.0) packages. Tidyverse packages (Wickham et al. 2019) were used for all data manipulation.

Microbial and dissolved thiamin congener statistical analyses

For beta diversity, the phyloseq package was used to generate microbial constrained analysis of principal coordinates (constrained by depth and sampling line) to maximize the variance associated with these variables and nonmetric multidimensional scaling (NMDS) ordinations at the genus level due to NMDS stress values being nearly zero at the ASV level. The microbiomeMarker (v1.2.2; Cao et al. 2022) and microViz (v.0.11.0; Barnett et al. 2021) packages were used with phyloseq objects to generate order-level stacked barplots with relative abundance calculated by depth and sampling line. The mia (v1.4.0; Ernst et al. 2023), ggtree (v3.4.4; Yu et al. 2016), and pheatmap (v1.0.12) packages were used to prepare phyloseq data for hierarchical clustering analyses, construct dendrograms, and for constructing a heatmap containing station and top genus (at least 70% of relative abundance per station) dendrograms, respectively. Complete-linkage agglomerative hierarchical clustering was performed based on Bray–Curtis dissimilarity matrices. Continuous variables used in linear regression as ordination vectors and for Pearson correlations in Supporting Information Table S1 (dissolved thiamin congeners, oxygen, density, chlorophyll *a*, irradiance, temperature, salinity, and transmissivity) analyses were transformed by Tukey's ladder of powers (Abdallah et al. 2017) with the rcompanion package (v2.4.34).

Analysis of microbiome composition with bias correction differential abundance was performed with the ANCOMBC package (v1.6.4; Lin and Peddada 2020) at the ASV level on

DADA2-processed reads, representing 99% of ASV relative abundances across samples, to relate ASV abundances with continuous dissolved thiamin congener concentrations. A total sum scaling-normalized count table of only analysis of microbiome composition with bias correction-identified differentially abundant ASVs (Supporting Information Table S2) was then used for microbiome multivariate associations with linear models (MaAsLin2; Mallick et al. 2021) analysis to find significant associations between ASV relative abundances and upwelling (Supporting Information Table S3), binned dissolved thiamin congeners, and depth (Supporting Information Tables S4, S5) (*see* MaAsLin2 data inputs and parameters in Supplemental Methods for details). Significant ASVs were identified based on a q value threshold of 0.25 (raw p and q values in Supporting Information Tables S3–S5). SAR11 oligotyping was performed with the otu2ot (Ramette and Buttigieg 2014) package, and ecotype nomenclature followed previously established taxonomy (Bolanos et al. 2022).

The vegan package (v2.6-4; Oksanen et al. 2016) was used for principal component analysis of dissolved thiamin congener concentrations, for permutational multivariate ANOVAs, to find significant metadata vectors ($p < 0.05$) that influenced the placement of samples onto ordination space (microbial community NMDS and dissolved thiamin congeners principal component analysis), and for partial Mantel tests to find Spearman correlations between Bray–Curtis microbial community dissimilarities and water column property Euclidean distance matrices (density and oxygen) with dissolved thiamin concentrations as a confounding variable. A mantel test (non-partial) was also performed to find a Spearman correlation between the microbial community dissimilarity and a depth distance matrix. Linear regression models were calculated with stepwise Akaike information criterion (AIC) (both directions) algorithms with the MASS (v7.3-60) package, and models were constructed with the stats (v4.2.1) package. Independent variables for each model were chosen to minimize multicollinearity and heteroscedasticity to ensure accurate model predictions (*see* Linear models section in Supplemental Methods for details on linear model assumptions testing). Kruskal–Wallis tests and Wilcoxon signed-rank tests, with the rstatix (v0.7.2) and ggpubr (v0.6.0) packages, were utilized to test for significance between dissolved thiamin compound concentration values within this study's CCE samples and between previously published marine dissolved thiamin compound concentrations.

Results

Unique chemical and environmental properties are found at each sampling line

Sampling lines (Navarro, the Gulf of Farallones [Farallones], Monterey Bay [Monterey], and Point Sur in Fig. 1a; hereby referred to as lines) displayed differences in temperature, water density, salinity, oxygen concentrations, and chlorophyll a levels between individual stations along coastal transects (Fig. 1b–e; Supporting Information Fig. S2). In general, water temperature tended to increase in stations further away from the coast and the opposite was true for density (Fig. 1b–e; Supporting Information Fig. S2). Navarro and Monterey stations contained the sharpest thermoclines and pycnoclines and several stations of these lines displayed limited temperature and density changes by depth (NAV-461, FAR-154, and SUR-105, -103, and -101) (Fig. 1b–e; Supporting Information Fig. S2). Salinity differed greatly in Navarro stations compared to all other lines and all stations generally displayed higher salinity in stations closer to the coast (Supporting Information Fig. S2).

Peaks in oxygen concentrations from station depth profiles were concurrent with peaks in chlorophyll a levels (Fig. 1b–e). Farallones and Navarro stations showed higher variabilities in oxygen concentrations (ml L^{-1}) and chlorophyll a levels (μg L^{-1}) than those of Monterey and Point Sur (interquartile concentration range values; Farallones: 3.01 and 9.38; Navarro: 2.56 and 4.71; Monterey: 2.15 and 1.31; Point Sur: 1.67 and 2.43, for oxygen and chlorophyll a, respectively). Navarro and Monterey were the only lines to contain stations with deep chlorophyll maxima (Fig. 1b–e). Chlorophyll a levels in the surface (4–6-m depth), intermediate (6–50 m and deep chlorophyll maxima), and deep (40–110 m) layers were highest in Farallones stations, particularly in FAR-139 (Fig. 1b–e). Upwelling fluctuated in intensity prior to, during, and following sampling across all four latitudes based on daily CUTI and biologically effective upwelling transport index measurements (Fig. 2a, b). Relative to the 2021 spring in the central CCE, Monterey stations exhibited strong upwelling (2.53 m^2 water s^{-1} and 49.2 mmol nitrate m^{-1} s^{-1}), Navarro & Point Sur stations displayed intermediate upwelling (1.38 and 1.00 m^2 water s^{-1} and 29.4 and 20.1 mmol nitrate m^{-1} s^{-1}, respectively), and Farallones stations displayed weak upwelling (0.24 m^2 water s^{-1} and 4.81 mmol nitrate m^{-1} s^{-1}). Monterey stations also had the deepest average mixed layers of any lines (Fig. 2c) and the deepest mixed layers of Monterey, Point Sur, and Farallones were at stations furthest from the coast (Fig. 2c).

Dissolved thiamin congener concentrations differ by sampling locations and upwelling intensities

The vertical distributions of dissolved thiamin congener concentrations varied between stations of the same line (Supporting Information Fig. S1 and Table S6; Fig. 3a). Interquartile concentration range values (displayed as numeric range) across all stations and depths were 7.70–118.0 pM thiamin, 1.88–7.46 pM HMP, 0.57–7.20 pM AmMP, 48.2–156.3 pM cHET, and 13.9–37.8 pM HET. Samples were binned into depth categories for dissolved thiamin congener and microbial analyses that included surface, intermediate, DCM, and deep samples (Fig. 3b). Wilcoxon Signed-Rank tests indicated a significant difference between surface layer and intermediate depth HMP concentrations, with median concentrations of 2.41 and 6.06 pM, respectively (Fig. 3b), but no other

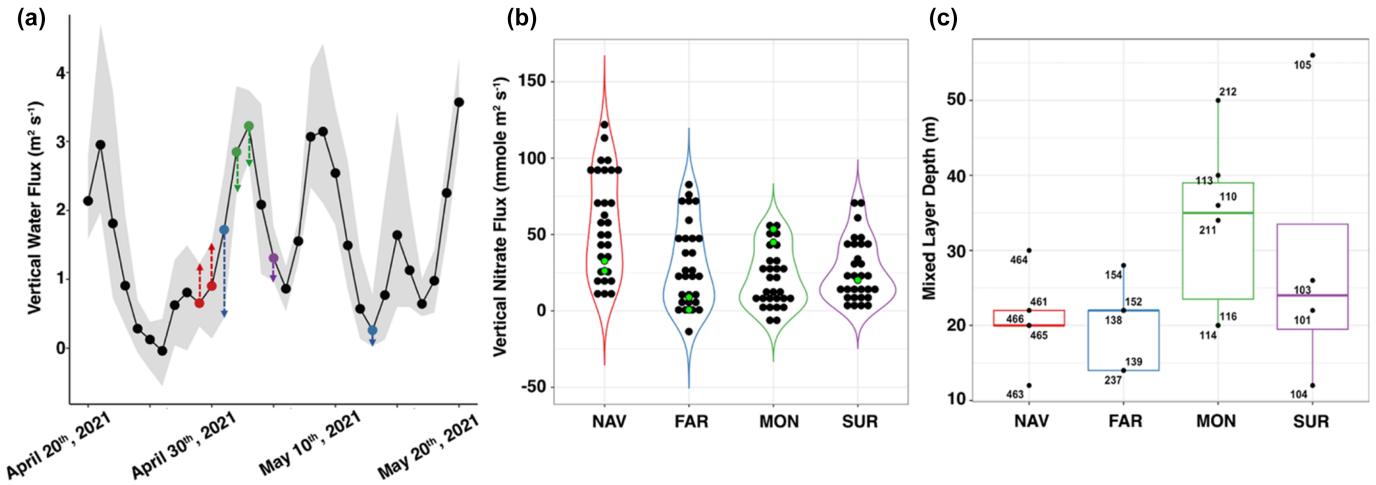

Fig. 2. Patterns of upwelling intensity and mixed layer depth. (**a**) Daily average Cumulative Upwelling Transport Index (CUTI) values, colored by sampling site (red = Navarro; blue = Farallones; green = Monterey; purple = Point Sur). Points indicate daily averages between all four lines. Dashed lines indicate discrete CUTI values of each line at their dates of sampling. Gray shading indicates daily maximum and minimum CUTI values across all four lines. (**b**) Daily biologically effective upwelling transport index values plotted by line and colored (bright green) by sampling time points. (**c**) Mixed layer depths by line and stations are indicated as numbers.

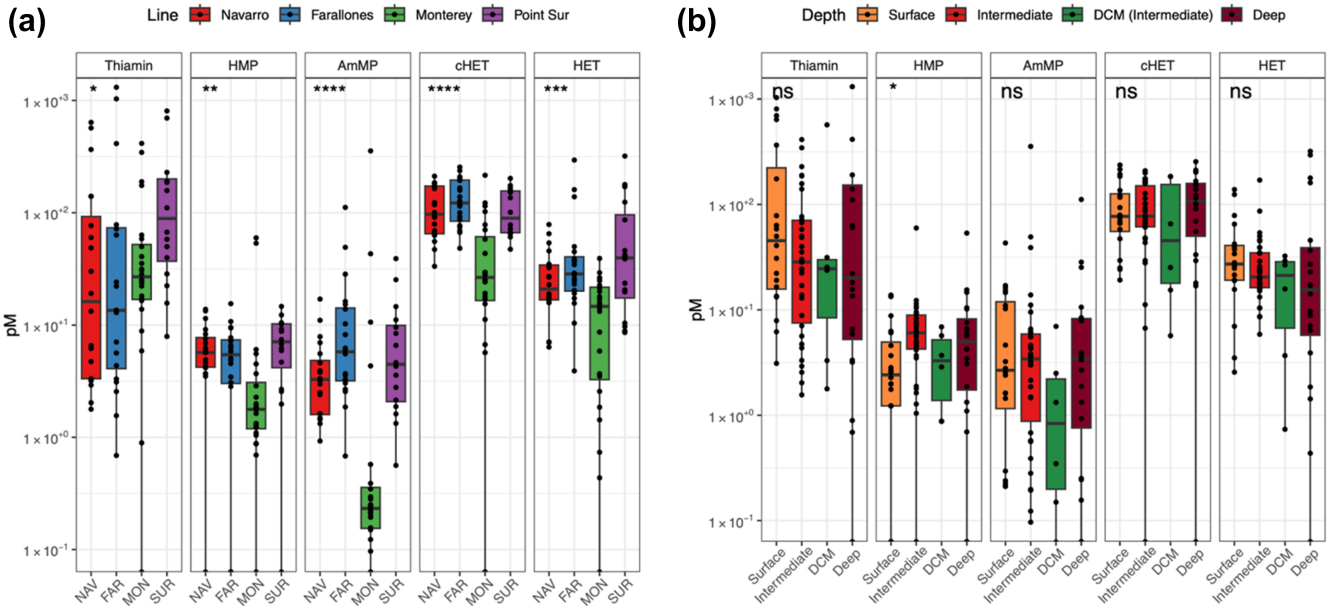

Fig. 3. Dissolved thiamin congener concentrations by sampling line and depth. (**a**) Line-by-line dissolved thiamin congener concentrations (log scale). (**b**) Dissolved thiamin congener concentrations (log scale) by each of the four discrete depth categories. Biosynthetic precursor compounds: 5-(2-hydroxyethyl)-4-methyl-1,3-thiazole-2-carboxylic acid (cHET) and 4-amino-5 hydroxymethyl-2-methylpyrimidine (HMP); abiotic degradation products: 4-amino-5-aminomethyl-2-methylpyrimidine (AmMP) and 4-methyl-5-thiazoleethanol (HET). Significant differences in concentrations between all lines (Kruskal–Wallis tests) indicated by asterisks: "ns" = not significant, $*p < 0.05$, $**p < 1 \times 10^{-2}$, $***p < 1 \times 10^{-3}$, $****p < 1 \times 10^{-4}$.

dissolved thiamin congeners significantly differed with depth. Significant differences were identified between lines by Kruskal–Wallis tests (Fig. 3a). Navarro, Farallones, and Point Sur lines displayed relatively consistent median concentrations of HMP (5.68, 5.44, and 7.09 pM, respectively), AmMP (3.28, 5.78, and 4.46 pM, respectively), cHET (97.1, 122.2, and 89.5 pM, respectively), and HET (20.9, 28.5, and 39.6 pM, respectively) while the Monterey line contained lower median concentrations of these dissolved thiamin congeners (1.78 pM HMP, 0.23 pM AmMP, 26.6 pM cHET, and 14.7 pM HET) (Fig. 3a). Median thiamin concentrations for each line were 16.2 pM (Navarro), 13.5 pM (Farallones), 26.8 pM (Monterey), and 88.9 pM (Point Sur), and were less variable between lines than other dissolved thiamin congeners (Fig. 3a).

The AIC-picked linear regression models displayed significant associations between thiamin congener concentrations (transformed), upwelling, and environmental factors (Table 1). Thiamin was the only congener that did not include CUTI as a predictor variable in its respective linear regression model (Table 1). Abiotic degradation products, HET and AmMP, were significantly and positively associated with concentrations of cHET and thiamin, respectively (Table 1). Linear regression results complemented those of dissolved thiamin congener differences by sampling line (Fig. 3a) because upwelling intensity did not significantly predict thiamin, while all other congeners were significantly and negatively associated with upwelling factors (HMP significant with density and oxygen, all other congeners with CUTI; Table 1). Based on Spearman correlations, thiamin concentrations did not significantly correlate with water column environmental properties, while cHET, AmMP, and HET all significantly positively correlated with chlorophyll *a* and cHET and AmMP negatively with transmissivity ($p < 0.05$; Supporting Information Table S1). Low concentrations of thiamin biosynthetic precursor compounds could therefore be an indication of the existence of strong upwelling, as portrayed in Monterey sample sites (Fig. 3a).

Dissolved thiamin congener concentrations from diverse marine ecosystems follow similar patterns to those within the central CCE

We compared the dissolved thiamin congener concentrations from this study to those measured in other globally distributed marine ecosystems to contextualize thiamin availability in the central CCE with that of other marine environments (Fig. 4). Across these diverse environments, which include multiple depth layers, we observed relatively uniform marine dissolved thiamin concentrations (interquartile concentration range = 14.8–96.7 pM; median = 31.5 pM) compared to thiamin precursor compounds and abiotic degradation products. The central CCE dissolved thiamin concentrations (median = 28.5 pM) only differed significantly from the data from Hood Canal, Washington, USA (median = 2.0 pM; Heal et al. 2014), and the Roskilde Fjord, Roskilde, Denmark (median 90.4; Bittner et al. 2024) (Fig. 4). However, the data from the Hood Canal are likely an underestimate due to low reported extraction efficiencies, substantial freshwater input, and poor circulation (Heal et al. 2014). The distributions reported in the southern region of the CCE (median = 40.0 pM; Sañudo-Wilhelmy et al. 2014; Monteverde et al. 2015), the Mediterranean Sea (median = 21.9 pM; Suffridge et al. 2018), the North Atlantic (median = 16.5 pM; Suffridge et al. 2020), and the Sargasso Sea (median = 16.0 pM; Carini et al. 2014) were not significantly different from the data in this study (Fig. 4). Dissolved HMP concentrations in the central CCE were significantly higher than those of the Mediterranean Sea and North Atlantic and significantly lower than those of the oligotrophic Sargasso Sea and the Roskilde Fjord (Fig. 4). The central CCE concentrations of cHET and HET were significantly higher than those of the North Atlantic and, in the case of HET, the

Table 1. Thiamin congener AIC-picked linear regression results.

Dependent variable	Independent variable	Estimate	SE (+/−)	Variable *p* value	Sig.	Model *p* value	Sig.	F-stat.	DOF	Adj. R^2
Thiamin	HMP	0.133	0.084	0.115	NS	0.046	*	2.80	3,74	0.07
Thiamin	cHET	0.015	0.009	0.114	NS	0.046	*	2.80	3,74	0.07
Thiamin	Irradiance	0.006	0.003	0.042	*	0.046	*	2.80	3,74	0.07
cHET	CUTI	−3.325	0.497	3.25×10^{-9}	***	3.25×10^{-9}	***	44.85	1,76	0.36
HMP	CUTI	−0.157	0.079	0.050	•	0.037	*	2.52	5,72	0.09
HMP	Thiamin	0.285	0.151	0.063	•	0.037	*	2.52	5,72	0.09
HMP	Density	-1.87×10^{-14}	8.74×10^{-15}	0.036	*	0.037	*	2.52	5,72	0.09
HMP	Oxygen	−0.191	0.082	0.023	*	0.037	*	2.52	5,72	0.09
HMP	Irradiance	−0.007	0.004	0.091	•	0.037	*	2.52	5,72	0.09
HET	CUTI	−0.155	0.069	0.027	*	1.08×10^{-5}	***	8.51	4,73	0.28
HET	HMP	0.156	0.093	0.098	•	1.08×10^{-5}	***	8.51	4,73	0.28
HET	cHET	0.031	0.013	0.015	*	1.08×10^{-5}	***	8.51	4,73	0.28
HET	Irradiance	0.006	0.003	0.066	•	1.08×10^{-5}	***	8.51	4,73	0.28
AmMP	CUTI	−0.135	0.031	3.55×10^{-5}	***	2.69×10^{-12}	***	28.3	3,74	0.52
AmMP	Thiamin	0.412	0.063	7.25×10^{-9}	***	2.69×10^{-12}	***	28.3	3,74	0.52
AmMP	DCM presence	−0.145	0.082	0.082	•	2.69×10^{-12}	***	28.3	3,74	0.52

AmMP, 4-amino-5-aminomethyl-2-methylpyrimidine; cHET, 5-(2-hydroxyethyl)-4-methyl-1,3-thiazole-2-carboxylic acid; CUTI, Cumulative Upwelling Transport Index; DCM, deep chlorophyll maximum; DOF, degrees of freedom; HMP, 4-amino-5 hydroxymethyl-2-methylpyrimidine; NS, not significant.
•$p < 0.10$; *$p < 0.05$; **$p < 0.01$; ***$p < 0.001$.

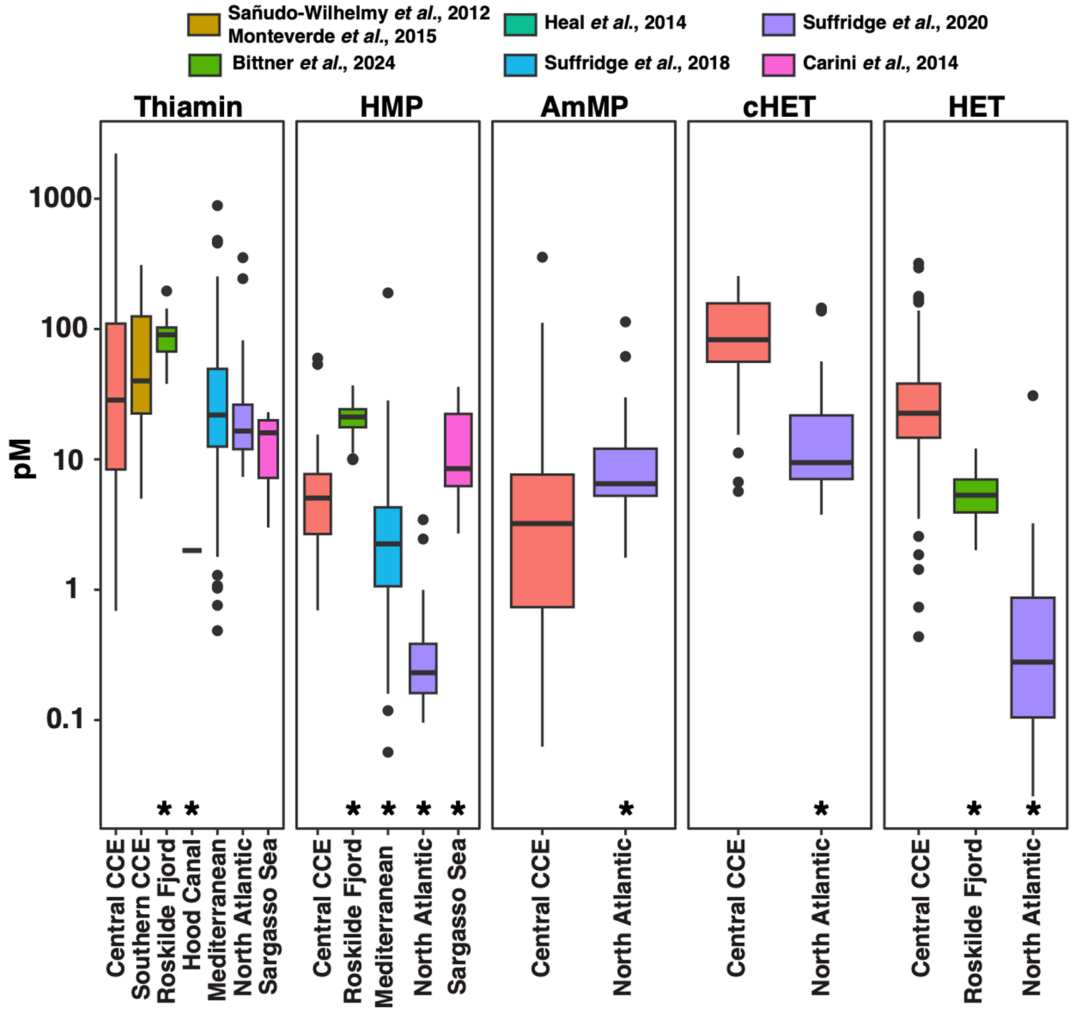

Fig. 4. Global comparison of dissolved thiamin congener concentrations in marine sites. The *y*-axis displays log scale pM concentrations, and columns are organized by individual thiamin congeners. Publication citations associated with each global dissolved thiamin congener sampling location (other than our data) are displayed in the key. Significant Wilcoxon signed-rank tests between central CCE samples and other marine locations are indicated by asterisks, individual significant pairwise *p* values (from left to right) are as follows: 1×10^{-3}, 4.5×10^{-4} (thiamin panel); 2×10^{-15}, 3.4×10^{-4}, 2.4×10^{-11}, 5×10^{-3} (HMP panel); 3.8×10^{-4} (AmMP panel); 1.8×10^{-8} (cHET panel); 1.1×10^{-11}, 2.4×10^{-11} (HET panel).

Roskilde Fjord (Fig. 4). The AmMP concentration was significantly lower in the central CCE than in the North Atlantic (Fig. 4).

Microbial community composition differs by sampling lines and depth, driven by dominant groups of bacteria, archaea, and algae

Prevalent bacteria, archaea, and algae display unique relative abundances in each sampling line and depth. Notably, algal relative abundances are based on chloroplast 16S rRNA read counts, rather than the chromosomal rRNA gene. Algal communities were predominantly composed of diatoms including Thalassiosirales, Bacillariales, Chaetocerotales, and Rhizosoleniales (Fig. 5a). Farallones, Navarro, Monterey, and Point Sur sites displayed particularly high relative abundances of Thalassiosirales, Chaetocerotales, and Corethrales diatoms, Prymnesiales and Phaeocystales haptophytes, and Naviculales (Point Sur) (Fig. 5a). Triceratiales diatoms also displayed heightened relative abundances in Point Sur and Farallones (Fig. 5a). Limited depth differences in algal relative abundances were observed, aside from heightened relative abundances of Phaeocystales and unclassified Prymnesiophyceae haptophytes in the deepest samples (Supporting Information Fig. S3A).

Across lines and depths, bacteria and archaea were primarily composed of Bacteroidota (Flavobacteriales and Chitinophagales), Proteobacteria (Alphaproteobacteria; Rhodobacterales, SAR11, and Gammaproteobacteria; Pseudomonadales), Crenarchaeota (Nitrosopumilales), Thermoplasmatota (Marine Group II), and Verrucomicrobiota (Verrucomicrobiales) (Fig. 5b). Flavobacterales and Rhodobacterales taxa showed high relative abundances in Navarro sites relative to other lines, and the opposite was true for Chitinophagales taxa (Fig. 5b).

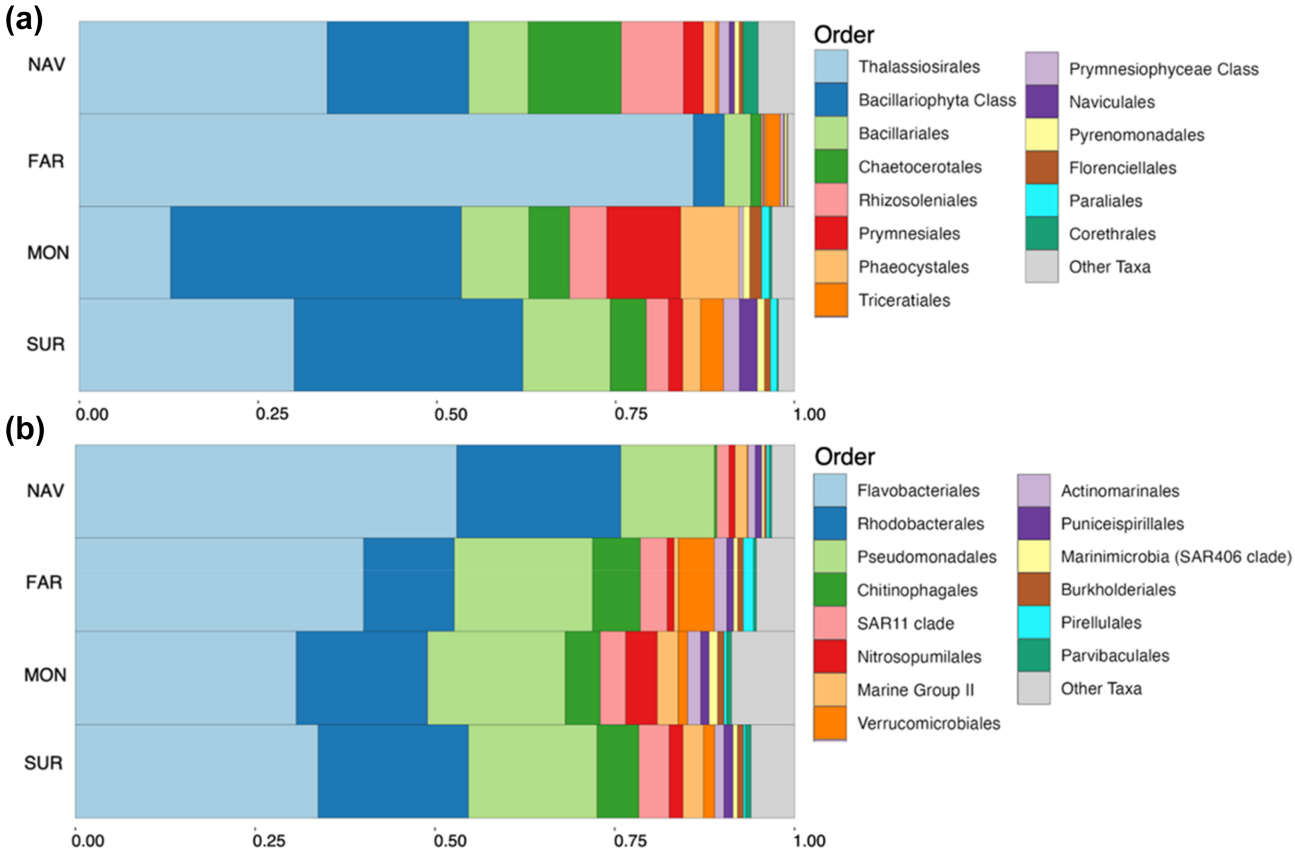

Fig. 5. Prevalent microbial orders by line. Stacked bar plots depicting the relative abundance of (**a**) algal and (**b**) bacterial and archaeal Orders. Colors and taxonomies are organized from high to low relative abundances (left to right). Relative abundances are averaged across stations and depths of each sampling line. The 15th most abundant taxonomic Orders were collapsed into the "Other taxa" category.

Farallones, Monterey, and Point Sur sites contained a similar composition of bacterial and archaeal orders with few exceptions: Nitrosopumilales and Verrucomicrobiales displayed high relative abundances in Monterey and Farallones sites, respectively (Fig. 5b). The deepest samples contained high relative abundances of Nitrosopumilales, Pseudomonadales, Marine Group II, Marinimicrobia (SAR406 clade), Microtrichales, SAR324 (Marine Group B), and rare taxa, and low relative abundances of Flavobacteriales, Rhodobacteriales, and Chitinophagales compared to other depths (Supporting Information Fig. S3B). Many taxa that displayed higher relative abundances in the deepest samples also showed high relative abundances in Monterey sample sites (Fig. 5b; Supporting Information Fig. S3B).

Microbial community composition and dissolved thiamin congener concentrations influence each other and are uniquely impacted by chemical and oceanographic factors

Bray–Curtis dissimilarities of bacterial, archaeal, and algal communities differed based on upwelling categories, line, and depth (permutational multivariate ANOVA $p = 0.001$ for all). The median Shannon diversity index did not greatly differ between the surface, intermediate, and DCM (if present) depths in any of the sampling lines, and only Monterey sites significantly differed by Kruskal–Wallis tests (Fig. 6a). The deepest samples in Monterey displayed the highest Shannon diversity of all depths across sampling lines (Fig. 6a). Constrained analysis of principal coordinates performed to maximize the community differences associated with the above variables explained 22.3% of variance on the principal axis and 12.9% of variance on the secondary axis (Fig. 6b). The deepest samples across sampling lines displayed similar microbial communities and differed greatly from surface, intermediate, and DCM samples (Fig. 6b). Based on the placement of samples in ordination space, the Farallones samples appeared to contain a unique community composition overall, as displayed in the constrained analysis of principal coordinates and NMDS plots (Fig. 6b,c).

Microbial community composition of each sampling line correlated with a multitude of environmental factors (Fig. 6c vectors of transformed variables; all $p < 0.05$), including dissolved thiamin congener concentrations (Fig. 6c vectors).

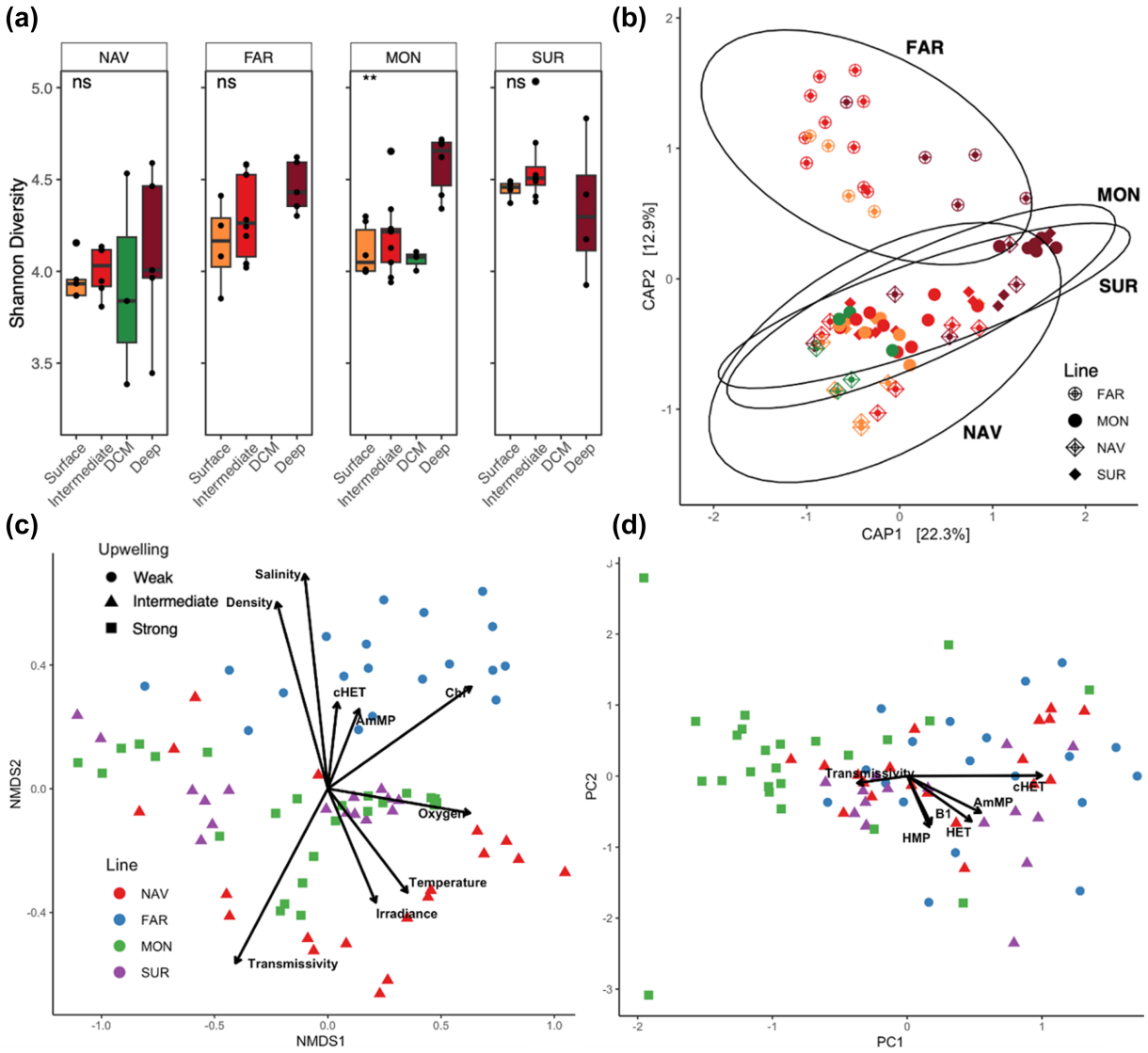

Fig. 6. Microbial and thiamin congener diversity. (**a**) Alpha diversity measured by the Shannon index (rarefied bacteria, archaea, and algae; amplicon sequence variant level) across depths for each sampling line. "ns" = not significant, $*p < 0.05$, $**p < 1 \times 10^{-2}$. (**b**) Constrained analysis of principal coordinates of the genus collapsed profiles for each sample, colored by depth categories. Each point corresponds to the genus-level microbiome at a discrete station and depth. Centroids correspond based on normalized multivariate distributions of genus relative abundances per line. (**c**) Nonmetric multidimensional scaling (NMDS) ordination (stress = 0.113) of genus-level microbiomes of discrete stations and depths with vectors ($p < 0.05$) indicating the influence of variables on the placement of samples in NMDS space. Samples are colored by line and shapes correspond to time periods of upwelling intensity. "Chl" = chlorophyll *a*. (**d**) Principal component analysis of dissolved thiamin congener profiles of each discrete station and depth with vectors ($p < 0.05$) indicating the influence of variables on the placement of samples in principal component analysis space. Samples are colored by line and shapes correspond to time periods of upwelling intensity.

AmMP and cHET concentrations each influenced the communities of Farallones sites (Fig. 6c), ostensibly contributing to their unique community composition. In addition to NMDS vectors (Fig. 6c), Partial Mantel test results provided evidence that upwelling-associated environmental factors (density and oxygen) influenced microbial community composition, independent of thiamin concentrations (thiamin included as confounding variable in partial Mantel test). Partial Mantel tests were performed on surface and intermediate (including DCM) depths to examine the influence of deep-water-associated environmental factors on shallower layer microbial communities, which could have an impact under strong upwelling due to the upward transport of water masses from deeper layers. Significant ($p < 0.05$) correlations existed between microbial Bray–Curtis dissimilarity matrices of genera in surface and intermediate depths and density and oxygen concentration differences (Spearman's correlation coefficients = 0.16 [density] and 0.08 [oxygen]; $p = 7 \times 10^{-4}$ [density] and 0.03 [oxygen]), indicating a high

influence of deep-water factors on intermediate-to-surface layer microbial communities.

Across all water depths, microbial community dissimilarity also increased concurrently with depth increases, based on Mantel (non-partial) tests between Bray–Curtis dissimilarity and water depth (Spearman's correlation coefficient = 0.17; $p = 1 \times 10^{-4}$). Similar to microbial communities, concentrations of the five dissolved thiamin congeners differed between sampling lines and temporally dependent upwelling intensities (Fig. 6d). Monterey differed the most in the dissolved thiamin congeners concentration profile compared to other lines (Fig. 6d; principal component 1 explained variance = 45.5%, principal component 2 explained variance = 0.67%), which was correlated with water transmissivity (Fig. 6d). These data display a potential link between microbial community composition, upwelling, and the dissolved pool of thiamin congeners (Fig. 6d).

Sampling stations cluster by abundant genera that influence dissolved thiamin congener concentrations

Sampling stations were clustered hierarchically based on Bray–Curtis dissimilarities of prevalent genera that comprised at least 70% of total relative abundance per station. A majority of these genera (25/38) contained ASVs that were differentially abundant ($p < 0.05$ in Supporting Information Table S2) with cHET (Fig. 7a; Supporting Information Table S2). Only *Roseibacillus* ASVs were differentially abundant with both thiazole moieties (Fig. 7a; Supporting Information Table S2). Fewer ASVs with low relative abundances were differentially abundant with HMP concentrations (2 total; OM27 clade and unclassified Desulfobacterota) and HET concentrations (4 total; *Roseibacillus* ASV [1], unclassified *Nitrincolaceae* [formerly *Oceanospirillaceae*] [2], and *Stappiaceae* [1]) (Supporting Information Table S2). A total of 43 ASVs were differentially abundant with cHET (Supporting Information Table S2), indicating

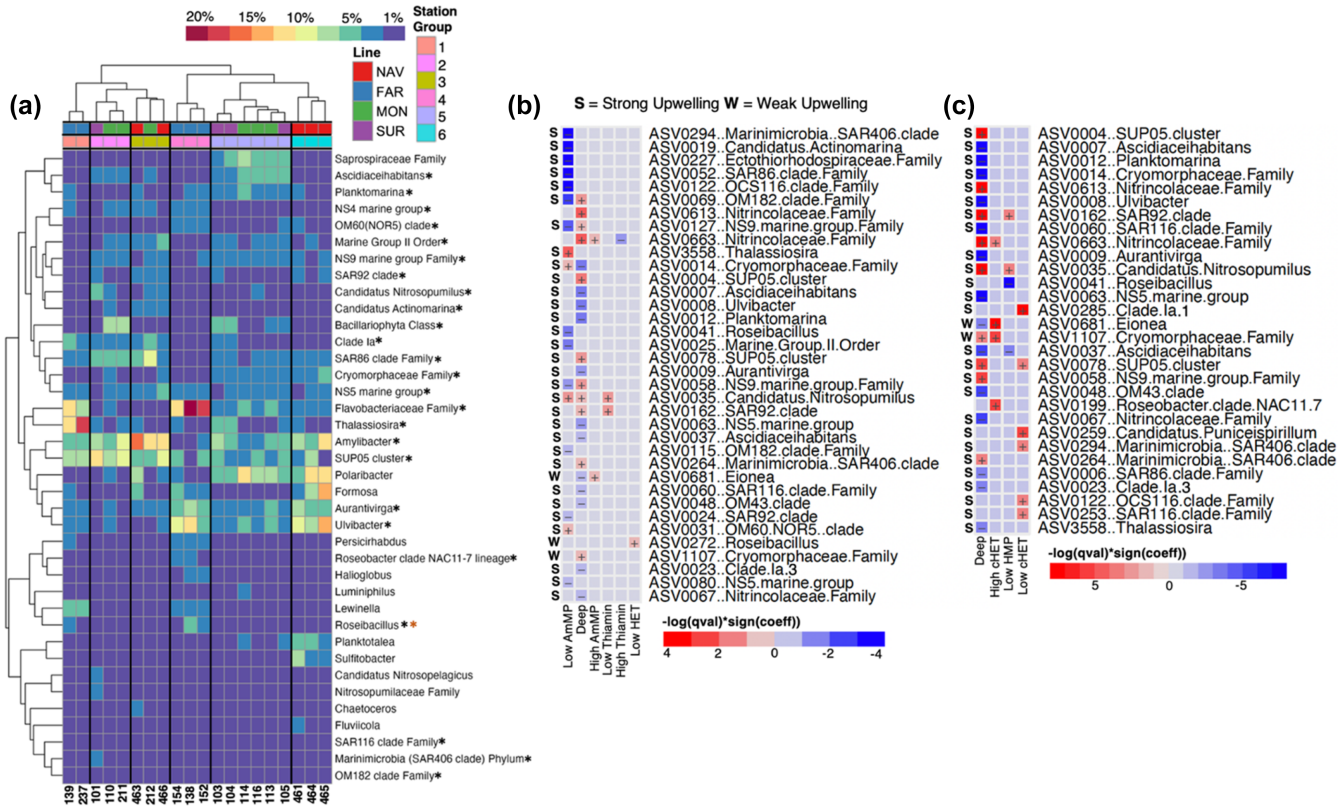

Fig. 7. Relative abundances of prevalent genera and significant ASV correlations with dissolved thiamin congeners. (**a**) Heatmap where *x*- and *y*-axes are ordered based on hierarchical clustering dendrograms derived from Bray–Curtis dissimilarities of the composition of abundant genera per station and those of abundant genera across stations. Station groups are synonymous with monophyletic groups of the dendrogram. Black asterisks indicate that the genus containing ASVs is differentially abundant with cHET concentrations. Orange asterisks indicate that the genus containing ASVs is differentially abundant with HET concentrations. (**b**, **c**) Differentially abundant ASVs were used to generate MaAsLin2 heatmaps displaying significant associations between binned sample depth, upwelling, thiamin (**b**), AmMP (**b**), and HET (**b**), HMP (**c**), and cHET (**c**). In both (**b**) and (**c**) panels, rows correspond to ASVs (with genera indicated) that are significantly associated with at least one *x*-axis variable. Upwelling associations are indicated by S and W for strong and weak upwelling, respectively (no letter indicates no association with upwelling). Negative associations (−) are indicated in blue and positive associations (+) are indicated in red, and the degree of significance (based on *q* values) is indicated by the color shade (*see* bottom keys). Categorical bins include: upwelling (weak, intermediate, strong), depth (surface, intermediate, deep), and thiamin congeners (low [< 25th percentile], intermediate [25th–75th percentile], and high [> 75th percentile]).

a considerable correlation between microbial communities and this compound. Collectively, the 54 ASVs that were differentially abundant differentially abundant ASVs (Supporting Information Table S2) represented 31.6% of total ASV relative abundance across all samples.

Significant correlations between relative abundances of differentially abundant ASVs and dissolved thiamin congener concentrations, upwelling intensity, and depth were identified by MaAsLin2 multivariate models. Nearly all of these taxa were significantly correlated ($q < 0.25$) with upwelling (48/54 differentially abundant ASVs; Supporting Information Fig. S4 and Table S3). In the first multivariate associations model (Fig. 7b), positively correlated taxa included *Nitrincolaceae*, *Eionea* (high AmMP bin), *Thalassiosira*, *Cryomorphaceae*, *Candidatus Nitrosopumilus*, and OM60 NOR5 clade (low AmMP bin), *Candidatus Nitrosopumilus* and SAR92 clade (low thiamin bin), and *Roseibacillus* (low HET) ASVs. Negatively correlated taxa (each genus containing 1 ASV unless indicated otherwise; Fig. 7b) included *Nitrincolaceae* (low thiamin bin) and *Marinimicrobia* SAR406 clade, *Candidatus Actinomarina*, *Ectothiorhodospiraceae*, SAR86, OCS116 clade, NS9 marine group (2 ASVs), *Roseibacillus*, Marine group II, OM182 clade, SAR92 clade, and NS5 marine group (low AmMP bin) ASVs. In the second multivariate associations model (Fig. 7c), positively correlated taxa included *Nitrincolaceae*, *Eionea*, *Cryomorphaceae*, and *Roseobacter* clade NAC11.7 (high cHET), SAR92 clade and *Candidatus Nitrosopumilus* (low HMP), and SAR11 clade 1a.1 ecotype, SUP05 cluster, *Candidatus Puniceispirillum*, *Marinimicrobia* SAR406 clade, OCS116 clade, and SAR116 clade ASVs (low cHET bin). Negatively correlated taxa (Fig. 7c) included *Roseibacillus* and *Ascidiaceihabitans* (low HMP bin) ASVs. A large portion of ASVs associated with dissolved thiamin congener bins also showed significant correlations with depth (Fig. 7b,c). These combined results provide further evidence that taxa whose relative abundances change with depth could uniquely influence dissolved thiamin congener concentrations, depending on upwelling intensity.

Discussion

Though site-specific environmental differences exist between sampling lines (sample site description in Methods), CUTI values showed consistent temporal upwelling patterns across the central CCE from late April to May (shaded gray range in Fig. 2a), indicating regionally stable temporal oscillations in upwelling. Our modeled upwelling data were consistent with the abnormally cool and upwelling-intense coastal conditions observed in 2021 in the central CCE, which were characterized by cool surface water temperatures and high chlorophyll *a* levels (Figs. 1, 2; Supporting Information Fig. S2) (Thompson et al. 2022). The general oceanographic patterns observed during 2021 were also consistent with those previously described for this region during this season, with increased temperatures and deeper mixed layer depths offshore, and higher salinity and density inshore (Santora et al. 2012). With oceanographic factors following previous trends, we hypothesized that microscale relationships between microbial populations and thiamin congeners would explain site-specific differences in thiamin congener availability and microbial community compositions.

Clear connections existed between CCE microbial community compositional changes, as a result of upwelling and water property changes from the upward transport of deep-water masses, and the net depletion or accumulation of thiamin congeners. Our data provide evidence that thiamin abiotic degradation products and biosynthetic precursors are depleted under strong-upwelling conditions while thiamin concentrations remained more stable with upwelling (Fig. 3a). Weak-upwelling Farallones stations contained higher pyrimidine and thiazole congener concentrations than strong-upwelling Monterey stations (Fig. 2a). Linear regression analysis also demonstrated that low concentrations of all congeners aside from thiamin were negatively associated with CUTI, indicating the potential for pyrimidine and thiazole congeners being more heavily trafficked by microbial communities than intact thiamin under upwelling conditions. Partial Mantel test results also indicated that microbial community changes in shallower water layers were influenced by deep-water-associated factors, providing evidence that thiamin congener depletion results from upwelling-driven microbial community alterations.

Our data also support the observation that changes to central CCE microbial community composition correlate with changes in dissolved thiamin congener concentrations, particularly thiazole compounds (Fig. 7a,b). Based on the limited depth differences in dissolved thiamin congener concentrations (Fig. 7b) and a large fraction of ASVs that significantly correlated with both changes in upwelling intensity and thiamin congeners (Fig. 7b,c), it is likely that upwelling-driven microbial community compositional changes result in alterations to the net exchange of thiamin congeners by microbes in the dissolved pool. Several key taxa appear to be involved in this hypothetical mechanism including *Thalassiosira*, which were abundant across sites in all sampling lines and are known thiamin prototrophs (Sañudo-Wilhelmy et al. 2014). While Farallones sites that exhibit weak upwelling contained the highest *Thalassiosira* relative abundances, one particular ASV was enriched with strong upwelling (Monterey sites) and with depth (ASV3558; Fig. 7b; Supporting Information Fig. S3). This trend was also displayed with SAR11 clade Ia ecotypes (Ia.1 and Ia.3), which were broadly distributed across all sample sites, yet specific ASVs were found only at Monterey sites (Supporting Information Fig. S5) and were significantly enriched with depth, strong upwelling, and at sites with low cHET concentrations (ASV0023 and ASV0285 in Fig. 7b; Supporting Information Fig. S4). SAR11 are known HMP auxotrophs, and relative abundances of unique SAR11 ASVs in strong-upwelling sites could have also been associated with the low HMP concentrations at Monterey stations

(Fig. 3). Overall, these data provide evidence that changes in relative abundance of specific ASVs have a meaningful influence on the dissolved pool of thiamin congeners.

SAR11 clade Ia ASVs are also known to vary based on upwelling-dependent nitracline depths in the Southern CCE (James et al. 2022). *Candidatus* Nitrosopumilus ASVs were enriched with depth, upwelling, and thiamin congeners (Fig. 7b), and can produce B vitamins (thiamin, B_2, B_5, B_6, and B_7; Santoro et al. 2015), potentially providing a thiamin source to auxotrophs like SAR11 taxa under upwelling conditions (Bayer et al. 2019). Relative abundances of *Eionea* and *Cryomorphaceae* ASVs further demonstrated the impact (or lack thereof) of upwelling on the relative abundances of individual ASVs that correlate with dissolved thiamin congener concentrations. These taxa were significantly enriched with both weak upwelling and high concentrations of AmMP and cHET (ASV0681 and ASV1107 in Fig. 7b), while one *Cryomorphaceae* ASV (ASV0014) was enriched with strong upwelling and low AmMP concentrations (Fig. 7b). Though high-level taxonomic annotations provide information on the genetic potential for microbes to cycle thiamin congeners (Sañudo-Wilhelmy et al. 2014; Paerl et al. 2018b), our data show that specific ASVs strongly correlate with dissolved thiamin congener concentrations in the upwelling-intense central CCE. More broadly, this could mean that strain-level variations in CCE microbial populations exert unique influences on thiamin congener trafficking.

Our results suggest that variations in upwelling intensity are associated with compositional and diversity alterations to microbial communities (Figs. 6a–c, 7b, c, and partial Mantel tests). These upwelling-associated microbial alterations could alter the net exchange of thiamin congeners between microbes and the dissolved pool. We hypothesize that the vertical transport of deep-water masses and microbes that is caused by strong upwelling leads to the depletion of thiamin congeners in the dissolved pool, likely due to an imbalance between microbial production and consumption (Fig. 8). This hypothesis is supported by the minimal site-by-site depth

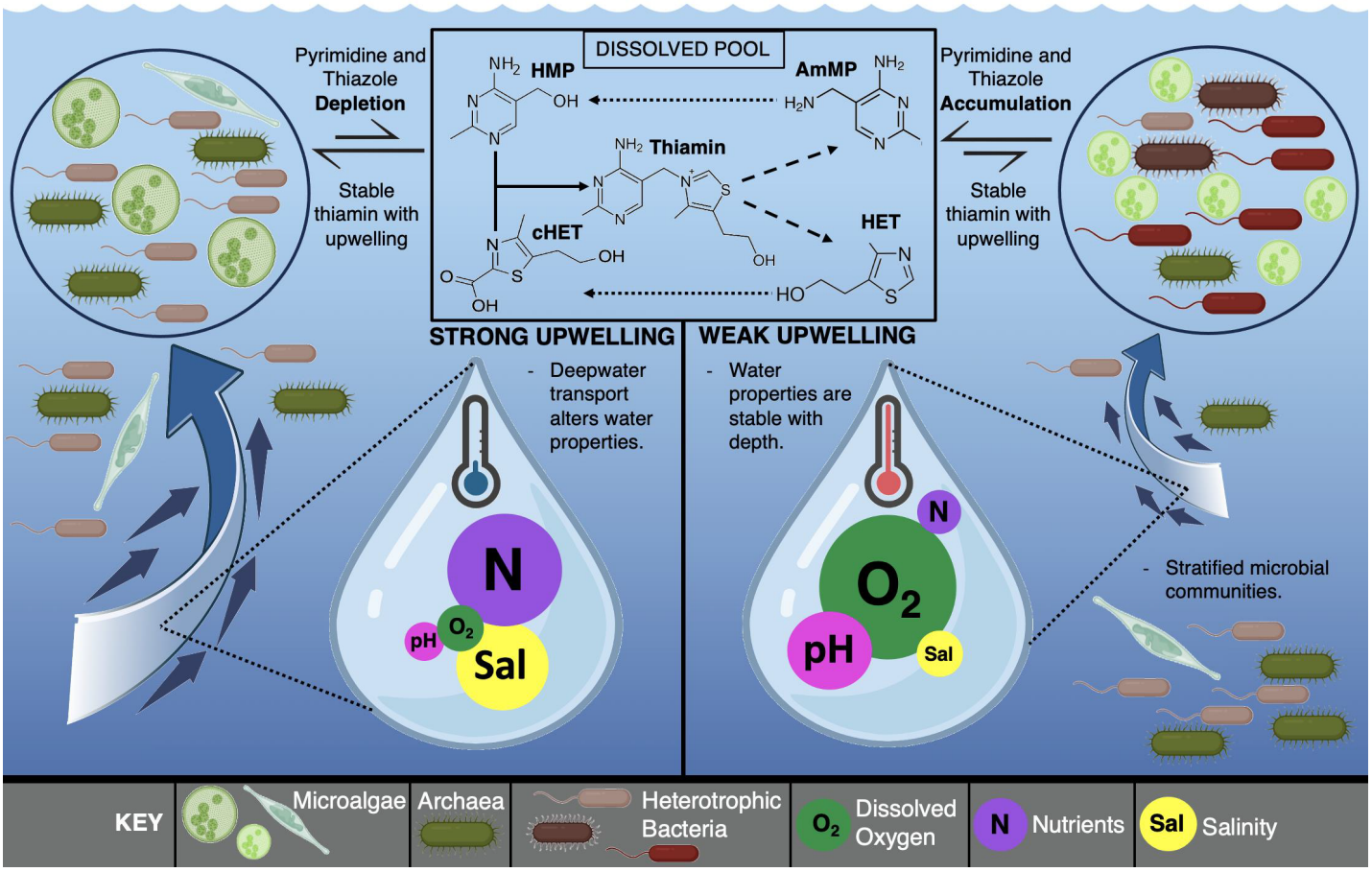

Fig. 8. Conceptual diagram of the influence of upwelling on microbial communities and dissolved thiamin congeners. Displays a water column with microbial communities (in circles) interacting with the dissolved pool of thiamin congeners in shallower layers. The direction of influence of microbial communities on thiazole (cHET and HET) and pyrimidine (HMP and AmMP) is indicated by reaction arrows. Vertical panels are separated by hypothetical upwelling intensity, indicated by magnitudes of blue arrows. Deep-water properties in each vertical panel are identified in water droplets and are purposely exaggerated to display differences.

changes in thiamin congener concentrations (Fig. 3b), while microbial communities and the influences of microbial populations on thiamin congeners varied greatly by depth (Supporting Information Figs. S3; Figs. 6a, b, 7b, c). Future research should examine if hypothetical imbalances in net thiamin congener exchange are caused by lower production by prototrophs, higher consumption by auxotrophs, or a combination of both factors under upwelling conditions. Our hypothesis is relevant to a rapidly changing CCE where major shifts in organismal diversity across trophic levels and regional intensified upwelling under climate change conditions have been projected (Xiu et al. 2018; Bograd et al. 2023). Water column acidity, deoxygenation, and nutrients have been modeled to increase commensurately with upwelling in the CCE (Cheresh and Fiechter 2020) and will likely have major impacts on microbial communities and concentrations of dissolved thiamin congeners (Fig. 8). Though our framework could broadly capture microbial and dissolved thiamin congener changes associated with upwelling, the impact of site-specific factors such as bathymetry, local weather, water mass mixing, and terrestrial inputs on microbial communities and dissolved thiamin congeners should also be considered. Based on our and global marine thiamin congener data (Fig. 4), it is also possible that the dissolved availability of intact thiamin is broadly less variable in marine ecosystems than pyrimidine and thiazole congeners. Previous work indicating genome-specific differences in thiamin auxotrophy states (Paerl et al. 2018b) supports this notion, as multitudes of microbial salvage strategies exist across global aquatic ecosystems to scavenge exogenous thiamin precursors for biosynthesis. We hypothesize that ASV- or strain-level changes in microbial populations with unique auxotrophy states are particularly influential on exogenous availabilities of thiamin precursors in marine ecosystems.

Conclusion

Thiamin is an essential coenzyme required by nearly all life on Earth, and assessing its microbially derived availability in rapidly changing CCE habitats is crucial to understanding the microbial ecology and food web stability of this ecosystem. Our data support our initial hypotheses that upwelling-associated alterations in springtime central CCE microbial community compositions influence dissolved thiamin congeners and that CCE thiamin congener concentrations are significantly different from those of other marine ecosystems. Heightened springtime upwelling may alter marine microbial communities in the CCE and influence the net exchange of dissolved thiamin congeners between microbial producers and consumers. Alterations to CCE microbial ecology could shift microbial communities toward states of disequilibria and potentially constrain concentrations of thiamin and biochemically related moieties in the dissolved pool. Further research will ascertain direct links between marine microbial communities and CCE biodiversity and identify how dissolved thiamin congeners influence food web stability from a full trophic level perspective.

Author Contributions

Project conceptualization was done by Kelly C. Shannon, Christopher P. Suffridge, Frederick S. Colwell, Rachel Johnson, and Nate Mantua. Samples were collected and research ship time was provided by Steven T. Lindley, John C. Field, and Nate Mantua. Analysis of samples was conducted by Kelly C. Shannon, Christopher P. Suffridge, Gillian St. John, Robin Gould, Christopher Hartzell, Hailey Matthews, and Elizabeth J. Brennan. Analysis of data was conducted by Kelly C. Shannon, Christopher P. Suffridge, Luis M. Bolaños, and Frederick S. Colwell. Kelly C. Shannon and Christopher P. Suffridge wrote the original manuscript draft, which was then reviewed and edited by Kelly C. Shannon, Luis M. Bolaños, Steven T. Lindley, John C. Field, Nate Mantua, Rachel Johnson, Carson Jeffres, Frederick S. Colwell, and Christopher P. Suffridge. Kelly C. Shannon was mentored by Frederick S. Colwell and Christopher P. Suffridge. Funding for this projected was provided by a grant to Christopher P. Suffridge.

Acknowledgments

We thank the Captain, Crew, and Science Party of the National Oceanic and Atmospheric Administration Ship R/V *Reuben Lasker* (cruise RL2103) for their assistance in sample collection. We thank Stephen Giovannoni for his support, mentorship, and use of his laboratory space. We thank Nastassia Patin for her helpful and constructive review of this manuscript. We thank Jeff Morré, Ryan Mueller, Byron Crump, and Jarrod Santora for their technical and scientific support. Finally, we thank the broader community of Salmonid Thiamin Deficiency Complex scientists for helpful and inspirational conversations that have shaped the direction of this research. This work was funded by the California Department of Fish and Wildlife grant Q2196012 to Christopher P. Suffridge. Additional personnel funding for Christopher P. Suffridge was provided by National Science Foundation grant DEB-1639033. Mass spectrometry instrumentation at the OSU Mass Spectrometry Center was supported by National Institutes of Health grant 1S10RR022589-1.

Conflict of Interest

The authors declare no conflicts of interest.

References

Abdallah, Z. S., L. Du, and G. I. Webb. 2017. "Data Preparation." In Encyclopedia of Machine Learning and Data Mining, edited by Sammut, C., Webb, G.I., 318–327. Boston,

MA: Springer. https://doi.org/10.1007/978-1-4899-7687-1_62.

Apprill, A., S. McNally, R. Parsons, and L. Weber. 2015. "Minor Revision to V4 Region SSU rRNA 806R Gene Primer Greatly Increases Detection of SAR11 Bacterioplankton." *Aquatic Microbial Ecology* 75: 129–137. https://doi.org/10.3354/ame01753.

Barnett, D. J. M., I. C. W. Arts, and J. Penders. 2021. "microViz: An R Package for Microbiome Data Visualization and Statistics." *Journal of Open Source Software* 6, no. 63: 3201. https://doi.org/10.21105/joss.03201.

Basant, K. D., and R. G. Arnold. 1973. "Chemistry of Thiamine Degradation in Food Products and Model Systems: A Review." *Journal of Agricultural and Food Chemistry* 21: 54–60. https://doi.org/10.1021/jf60185a004.

Bayer, B., R. L. Hansman, M. J. Bittner, et al. 2019. "Ammonia-Oxidizing Archaea Release a Suite of Organic Compounds Potentially Fueling Prokaryotic Heterotrophy in the Ocean." *Environmental Microbiology* 21: 4062–4075. https://doi.org/10.1111/1462-2920.14755.

Bertrand, E. M., and A. E. Allen. 2012. "Influence of Vitamin B Auxotrophy on Nitrogen Metabolism in Eukaryotic Phytoplankton." *Frontiers in Microbiology* 3: 375. https://doi.org/10.3389/fmicb.2012.00375.

Bittner, M. J., C. C. Bannon, E. Rowland, et al. 2024. "New Chemical and Microbial Perspectives on Vitamin B1 and Vitamer Dynamics of a Coastal System." *ISME Communications* 4, no. 1: ycad016. https://doi.org/10.1093/ismeco/ycad016.

Bograd, S. J., M. G. Jacox, E. L. Hazen, et al. 2023. "Climate Change Impacts on Eastern Boundary Upwelling Systems." *Annual Review of Marine Science* 15: 303–328. https://doi.org/10.1146/annurev-marine-032122-021945.

Bolanos, L. M., K. Tait, P. J. Somerfield, et al. 2022. "Influence of Short and Long Term Processes on SAR11 Communities in Open Ocean and Coastal Systems." *ISME Communications* 2: 116. https://doi.org/10.1038/s43705-022-00198-1.

Callahan, B. J., P. J. McMurdie, M. J. Rosen, A. W. Han, A. J. Johnson, and S. P. Holmes. 2016. "DADA2: High-Resolution Sample Inference from Illumina Amplicon Data." *Nature Methods* 13: 581–583. https://doi.org/10.1038/nmeth.3869.

Cao, Y., Q. Dong, D. Wang, P. Zhang, Y. Liu, and C. Niu. 2022. "microbiomeMarker: An R/Bioconductor Package for Microbiome Marker Identification and Visualization." *Bioinformatics* 38: 4027–4029. https://doi.org/10.1093/bioinformatics/btac438.

Carini, P., E. O. Campbell, J. Morré, et al. 2014. "Discovery of a SAR11 Growth Requirement for Thiamin's Pyrimidine Precursor and Its Distribution in the Sargasso Sea." *The ISME Journal* 8: 1727–1738. https://doi.org/10.1038/ismej.2014.61.

Carlucci, A. F., S. B. Silbernagel, and P. M. McNally. 1969. "Influence of Temperature and Solar Radiation on Persistence of Vitamin B12, Thiamine, and Biotin in Seawater." *Journal of Phycology* 5: 302–305. https://doi.org/10.1111/j.1529-8817.1969.tb02618.x.

Carter, G. S., and M. C. Gregg. 2002. "Intense, Variable Mixing near the Head of Monterey Submarine Canyon." *Journal of Physical Oceanography* 32: 95–110. https://doi.org/10.1175/1520-0485(2002)032%3C3145:IVMNTH%3E2.0.CO;2.

Checkley, D. M., and J. A. Barth. 2009. "Patterns and Processes in the California Current System." *Progress in Oceanography* 83: 49–64. https://doi.org/10.1016/j.pocean.2009.07.028.

Cheresh, J., and J. Fiechter. 2020. "Physical and Biogeochemical Drivers of Alongshore pH and Oxygen Variability in the California Current System." *Geophysical Research Letters* 47, no. 19: e2020GL089553. https://doi.org/10.1029/2020GL089553.

Closek, C. J., J. A. Santora, H. A. Starks, et al. 2019. "Marine Vertebrate Biodiversity and Distribution within the Central California Current Using Environmental DNA (eDNA) Metabarcoding and Ecosystem Surveys." *Frontiers in Marine Science* 6: 732. https://doi.org/10.3389/fmars.2019.00732.

Cornec, M., H. Claustre, A. Mignot, et al. 2021. "Deep Chlorophyll Maxima in the Global Ocean: Occurrences, Drivers and Characteristics." *Global Biogeochemical Cycles* 35: e2020GB006759. https://doi.org/10.1029/2020GB006759.

Countway, P. D., P. D. Vigil, A. Schnetzer, S. D. Moorthi, and D. A. Caron. 2010. "Seasonal Analysis of Protistan Community Structure and Diversity at the USC Microbial Observatory (San Pedro Channel, North Pacific Ocean)." *Limnology and Oceanography* 55: 2381–2396. https://doi.org/10.4319/lo.2010.55.6.2381.

Croft, M. T., M. J. Warren, and A. G. Smith. 2006. "Algae Need their Vitamins." *Eukaryotic Cell* 5: 1175–1183. https://doi.org/10.1128/EC.00097-06.

Davis, N. M., D. M. Proctor, S. P. Holmes, D. A. Relman, and B. J. Callahan. 2018. "Simple Statistical Identification and Removal of Contaminant Sequences in Marker-Gene and Metagenomics Data." *Microbiome* 6: 226. https://doi.org/10.1186/s40168-018-0605-2.

de Boyer Montégut, C., G. Madec, A. S. Fischer, A. Lazar, and D. Iudicone. 2004. "Mixed Layer Depth over the Global Ocean: An Examination of Profile Data and a Profile-Based Climatology." *Journal of Geophysical Research: Oceans* 109, no. C12: 2004JC002378. https://doi.org/10.1029/2004JC002378.

Decelle, J., S. Romac, R. F. Stern, et al. 2015. "PhytoREF: A Reference Database of the Plastidial 16S rRNA Gene of Photosynthetic Eukaryotes with Curated Taxonomy." *Molecular Ecology Resources* 15: 1435–1445. https://doi.org/10.1111/1755-0998.12401.

Ernst, F., S. Shetty, T. Borman, and L. Lahti. 2023. mia: Microbiome Analysis. R package version 1.14. https://github.com/microbiome/mia.

Ewels, P., M. Magnusson, S. Lundin, and M. Kaller. 2016. "MultiQC: Summarize Analysis Results for Multiple Tools

and Samples in a Single Report." *Bioinformatics* 32: 3047–3048. https://doi.org/10.1093/bioinformatics/btw354.

Field, J. C., R. R. Miller, J. A. Santora, et al. 2021. "Spatiotemporal Patterns of Variability in the Abundance and Distribution of Winter-Spawned Pelagic Juvenile Rockfish in the California Current." *PLoS One* 16, no. 5:e0251638. https://doi.org/10.1371/journal.pone.0251638.

Gold, K. 1968. "Some Factors Affecting the Stability of Thiamine." *Limnology and Oceanography* 13: 185–188. https://doi.org/10.4319/lo.1968.13.1.0185.

Gutowska, M. A., B. Shome, S. Sudek, et al. 2017. "Globally Important Haptophyte Algae Use Exogenous Pyrimidine Compounds More Efficiently Than Thiamin." *MBio* 8, no. 5: e01459-17. https://doi.org/10.1128/mBio.01459-17.

Heal, K. R., L. T. Carlson, A. H. Devol, et al. 2014. "Determination of Four Forms of Vitamin B12 and Other B Vitamins in Seawater by Liquid Chromatography/Tandem Mass Spectrometry." *Rapid Communications in Mass Spectrometry* 28: 2398–2404. https://doi.org/10.1002/rcm.7040.

Hickey, B. M. 1995. "Coastal Submarine Canyons." In Topographic Effects in the Ocean, edited by P. Muller and D. Henderson, 95–110. Manoa: SOEST Special Publication, University of Hawaii.

Hickey, B. M., and N. S. Banas. 2003. "Oceanography of the U.S. Pacific Northwest Coastal Estuaries with Application to Coastal Ecology." *Estuaries* 26: 1010–1031. https://doi.org/10.1007/BF02803360.

Huyer, A. 1983. "Coastal Upwelling in the California Current System." *Progress in Oceanography* 12: 259–284. https://doi.org/10.1016/0079-6611(83)90010-1.

Jacox, M. G., C. A. Edwards, E. L. Hazen, and S. J. Bograd. 2018. "Coastal Upwelling Revisited: Ekman, Bakun, and Improved Upwelling Indices for the U.S. West Coast." *Journal of Geophysical Research: Oceans* 123: 7332–7350. https://doi.org/10.1029/2018JC014187.

James, C. C., A. D. Barton, L. Z. Allen, et al. 2022. "Influence of Nutrient Supply on Plankton Microbiome Biodiversity and Distribution in a Coastal Upwelling Region." *Nature Communications* 13: 2448. https://doi.org/10.1038/s41467-022-30139-4.

Jurgenson, C. T., T. P. Begley, and S. E. Ealick. 2009. "The Structural and Biochemical Foundations of Thiamin Biosynthesis." *Annual Review of Biochemistry* 78: 569–603. https://doi.org/10.1146/annurev.biochem.78.072407.102340.

Kraft, C. E., and E. R. Angert. 2017. "Competition for Vitamin B1(Thiamin) Structures Numerous Ecological Interactions." *Quarterly Review of Biology* 92: 151–168. https://doi.org/10.1086/692168.

Lin, H., and S. D. Peddada. 2020. "Analysis of Compositions of Microbiomes with Bias Correction." *Nature Communications* 11: 3514. https://doi.org/10.1038/s41467-020-17041-7.

Mallick, H., A. Rahnavard, L. J. McIver, et al. 2021. "Multivariable Association Discovery in Population-Scale Meta-Omics Studies." *PLoS Computational Biology* 17, no. 11: e1009442. https://doi.org/10.1371/journal.pcbi.1009442.

McKnight, D. T., R. Huerlimann, D. S. Bower, et al. 2018. "Methods for Normalizing Microbiome Data: An Ecological Perspective." *Methods in Ecology and Evolution* 10: 389–400. https://doi.org/10.1111/2041-210X.13115.

McMurdie, P. J., and S. Holmes. 2013. "Phyloseq: An R Package for Reproducible Interactive Analysis and Graphics of Microbiome Census Data." *PLoS One* 8: e61217. https://doi.org/10.1371/journal.pone.0061217.

Minich, J. J., J. G. Sanders, A. Amir, G. Humphrey, J. A. Gilbert, and R. Knight. 2019. "Quantifying and Understanding Well-to-Well Contamination in Microbiome Research." *mSystems* 4, no. 4: e00186-19. https://doi.org/10.1128/mSystems.00186-19.

Monteverde, D. R., L. Gomez-Consarnau, L. Cutter, L. Chong, W. Berelson, and S. A. Sanudo-Wilhelmy. 2015. "Vitamin B1 in Marine Sediments: Pore Water Concentration Gradient Drives Benthic Flux with Potential Biological Implications." *Frontiers in Microbiology* 6: 434. https://doi.org/10.3389/fmicb.2015.00434.

Oksanen, J., F. G. Blanchet, M. Friendly, et al. 2016. Vegan: Community Ecology Package. R package version 2.7-0. https://github.com/vegandevs/vegan.

Paerl, R. W., E. M. Bertrand, E. Rowland, et al. 2018*a*. "Carboxythiazole Is a Key Microbial Nutrient Currency and Critical Component of Thiamin Biosynthesis." *Scientific Reports* 8: 5940. https://doi.org/10.1038/s41598-018-24321-2.

Paerl, R. W., F. Y. Bouget, J. C. Lozano, et al. 2017. "Use of Plankton-Derived Vitamin B1 Precursors, Especially Thiazole-Related Precursor, by Key Marine Picoeukaryotic Phytoplankton." *The ISME Journal* 11: 753–765. https://doi.org/10.1038/ismej.2016.145.

Paerl, R. W., J. Sundh, D. Tan, et al. 2018*b*. "Prevalent Reliance of Bacterioplankton on Exogenous Vitamin B1 and Precursor Availability." *Proceedings of the National Academy of Sciences* 115: E10447–E10456. https://doi.org/10.1073/pnas.1806425115.

Parada, A. E., D. M. Needham, and J. A. Fuhrman. 2016. "Every Base Matters: Assessing Small Subunit rRNA Primers for Marine Microbiomes with Mock Communities, Time Series and Global Field Samples." *Environmental Microbiology* 18: 1403–1414. https://doi.org/10.1111/1462-2920.13023.

Quast, C., E. Pruesse, P. Yilmaz, et al. 2013. "The SILVA Ribosomal RNA Gene Database Project: Improved Data Processing and Web-Based Tools." *Nucleic Acids Research* 41: D590–D596. https://doi.org/10.1093/nar/gks1219.

Ramette, A., and P. L. Buttigieg. 2014. "The R Package otu2ot for Implementing the Entropy Decomposition of Nucleotide Variation in Sequence Data." *Frontiers in Microbiology* 5: 601. https://doi.org/10.3389/fmicb.2014.00601.

RStudio Team. 2020. Integrated Development for R. Boston, MA: RStudio.

Santora, J. A., J. C. Field, I. D. Schroeder, K. M. Sakuma, B. K. Wells, and W. J. Sydeman. 2012. "Spatial Ecology of Krill, Micronekton and Top Predators in the Central California Current: Implications for Defining Ecologically Important Areas." *Progress in Oceanography* 106: 154–174. https://doi.org/10.1016/j.pocean.2012.08.005.

Santora, J. A., I. D. Schroeder, S. J. Bograd, et al. 2021. "Pelagic Biodiversity, Ecosystem Function, and Services." *Oceanography* 34: 16–37. https://www.jstor.org/stable/27085036.

Santoro, A. E., C. L. Dupont, R. A. Richter, et al. 2015. "Genomic and Proteomic Characterization of '*Candidatus Nitrosopelagicus* brevis': An Ammonia-Oxidizing Archaeon from the Open Ocean." *Proceedings of the National Academy of Sciences of the United States of America* 112: 1173–1178. https://doi.org/10.1073/pnas.1416223112.

Santoro, A. E., N. J. Nidzieko, G. L. van Dijken, K. R. Arrigo, and A. B. Boehma. 2010. "Contrasting Spring and Summer Phytoplankton Dynamics in the Nearshore Southern California Bight." *Limnology and Oceanography* 55: 264–278. https://doi.org/10.4319/lo.2010.55.1.0264.

Sanudo-Wilhelmy, S. A., L. S. Cutter, R. Durazo, et al. 2012. "Multiple B-Vitamin Depletion in Large Areas of the Coastal Ocean." *Proceedings of the National Academy of Sciences of the United States of America* 109: 14041–14045. https://doi.org/10.1073/pnas.1208755109.

Sañudo-Wilhelmy, S. A., L. Gómez-Consarnau, C. Suffridge, and E. A. Webb. 2014. "The Role of B Vitamins in Marine Biogeochemistry." *Annual Review of Marine Science* 6: 339–367. https://doi.org/10.1146/annurev-marine-120710-100912.

Steger, J. M., F. B. Schwing, C. A. Collins, L. K. Rosenfeld, N. Garfield, and E. Gezgin. 2000. "The Circulation and Water Masses in the Gulf of the Farallones." *Deep Sea Research Part II: Topical Studies in Oceanography* 47: 907–946. https://doi.org/10.1016/S0967-0645(99)00131-9.

Suffridge, C., L. Cutter, and S. A. Sañudo-Wilhelmy. 2017. "A New Analytical Method for Direct Measurement of Particulate and Dissolved B-Vitamins and Their Congeners in Seawater." *Frontiers in Marine Science* 4. https://doi.org/10.3389/fmars.2017.00011.

Suffridge, C. P., L. M. Bolaños, K. Bergauer, et al. 2020. "Exploring Vitamin B1 Cycling and Its Connections to the Microbial Community in the North Atlantic Ocean." *Frontiers in Marine Science* 7: 606342. https://doi.org/10.3389/fmars.2020.606342.

Suffridge, C. P., L. Gómez-Consarnau, D. R. Monteverde, et al. 2018. "B Vitamins and Their Congeners as Potential Drivers of Microbial Community Composition in an Oligotrophic Marine Ecosystem." *Journal of Geophysical Research: Biogeosciences* 123: 2890–2907. https://doi.org/10.1029/2018JG004554.

Suffridge, C. P., K. C. Shannon, H. Matthews, et al. 2023. "Connecting Thiamine Availability to the Microbial Community Composition in Chinook Salmon Spawning Habitats of the Sacramento River Basin." *Environmental Microbiology* 90: e01760-23. https://doi.org/10.1128/aem.01760-23.

Thompson, A. R., E. P. Bjorkstedt, S. J. Bograd, et al. 2022. "State of the California Current Ecosystem in 2021: Winter Is Coming?" *Frontiers in Marine Science* 9: 2296–7745. https://doi.org/10.3389/fmars.2022.958727.

Vander Woude, A. J., J. L. Largier, and R. M. Kudela. 2006. "Nearshore Retention of Upwelled Waters North and South of Point Reyes (Northern California)—Patterns of Surface Temperature and Chlorophyll Observed in CoOP WEST." *Deep Sea Research Part II: Topical Studies in Oceanography* 53: 2985–2998. https://doi.org/10.1016/j.dsr2.2006.07.003.

Venrick, E. L. 2009. "Floral Patterns in the California Current: The Coastal-Offshore Boundary Zone." *Journal of Marine Research* 67: 89–111. https://doi.org/10.1357/002224009788597917.

Wickham, H. 2009. ggplot2: Elegant Graphics for Data Analysis. New York: SpringerVerlag.

Wickham, H., M. Averick, J. Bryan, et al. 2019. "Welcome to the Tidyverse." *Journal of Open Source Software* 4: 1686. https://doi.org/10.21105/joss.01686.

Wienhausen, G., M. J. Bittner, and R. W. Paerl. 2022. "Key Knowledge Gaps to Fill at the Cell-to-Ecosystem Level in Marine B-Vitamin Cycling." *Frontiers in Marine Science* 9: 876726. https://doi.org/10.3389/fmars.2022.876726.

Wienhausen, G., B. E. Noriega-Ortega, J. Niggemann, T. Dittmar, and M. Simon. 2017. "The Exometabolome of Two Model Strains of the Roseobacter Group: A Marketplace of Microbial Metabolites." *Frontiers in Microbiology* 8: 1985. https://doi.org/10.3389/fmicb.2017.01985.

Xiu, P., F. Chai, E. N. Curchitser, and F. S. Castruccio. 2018. "Future Changes in Coastal Upwelling Ecosystems with Global Warming: The Case of the California Current System." *Scientific Reports* 8: 2866. https://doi.org/10.1038/s41598-018-21247-7.

Yu, G., D. K. Smith, H. Zhu, Y. Guan, T. T. Y. Lam, and G. McInerny. 2016. "Ggtree: An R Package for Visualization and Annotation of Phylogenetic Trees with Their Covariates and Other Associated Data." *Methods in Ecology and Evolution* 8: 28–36. https://doi.org/10.1111/2041-210X.12628.

Zhang, K., J. Bian, Y. Deng, et al. 2016. "Lyme Disease Spirochaete Borrelia Burgdorferi Does Not Require Thiamin." *Nature Microbiology* 2: 16213.https://doi.org/10.1038/nmicrobiol.2016.213.

Zhou, J., J. G. Izett, C. A. Edwards, P. Damien, F. Kessouri, and J. C. McWilliams. 2023. "Modeling the Dispersal of the San Francisco Bay Plume over the Northern and Central

California Shelf." *Estuarine, Coastal and Shelf Science* 287: 108336. https://doi.org/10.1016/j.ecss.2023.108336.

Submitted 19 April 2024
Revised 12 September 2024
Accepted 17 February 2025

Supporting Information

Additional Supporting Information may be found in the online version of this article.